Research Article | Vol. 25, No. 11 | 29 May 2017 | OPTICS EXPRESS 12493

Optics EXPRESS

# Multiple-DWDM-channel heralded single-photon source based on a periodically poled lithium niobate waveguide

TONG XIANG,[1,2] YUANHUA LI,[1,2] YUANLIN ZHENG,[1,2] AND XIANFENG CHEN[1,2,*]

[1]*State Key Laboratory of Advanced Optical Communication Systems and Networks, School of Physics and Astronomy, Shanghai Jiao Tong University, Shanghai 200240, China*
[2]*Key Laboratory for Laser plasma (Ministry of Education), Collaborative Innovation Center of IFSA (CICIFSA), Shanghai Jiao Tong University, Shanghai 200240, China*
**xfchen@sjtu.edu.cn*

**Abstract:** We report on the experimental realization of a multiple-DWDM-channel heralded single-photon source in a periodically poled lithium niobate waveguide. Our single photon at the telecom wavelength covers more than 40 channels of the ITU grid. All channels have virtually identical efficiencies, and the multi-photon emission probability is reduced by a factor up to more than 150 compared to a Poissonian light source. Together with the all-fiber structure, all these advantages make our heralded single-photon source suitable for real-world quantum networks. The implementation with a 50 MHz pulsed laser provides a data rate compatible with current quantum communication systems, while being able to be pumped at higher repetition rates.

© 2017 Optical Society of America

**OCIS codes:** (190.0190) Nonlinear optics; (270.5565) Quantum communications.

## References and links

1. C. H. Bennett, G. Brassard, C. Crépeau, R. Jozsa, A. Peres, and W. K. Wootters, “Teleporting an unknown quantum state via dual classical and Einstein-Podolsky-Rosen channels,” Phys. Rev. Lett. **70**(13), 1895–1899 (1993).
2. Q. Wang, X. B. Wang, and G. C. Guo, “Practical decoy-state method in quantum key distribution with a heralded single-photon source,” Phys. Rev. A **75**(1), 012312 (2007).
3. K. Takemoto, Y. Nambu, T. Miyazawa, Y. Sakuma, T. Yamamoto, S. Yorozu, and Y. Arakawa, “Quantum key distribution over 120 km using ultrahigh purity single-photon source and superconducting single-photon detectors,” Sci. Rep. **5**(1), 14383 (2015).
4. Q. C. Sun, Y. L. Mao, S. J. Chen, W. Zhang, Y. F. Jiang, Y. B. Zhang, W. J. Zhang, S. Miki, T. Yamashita, H. Terai, X. Jiang, T. Y. Chen, L. X. You, X. F. Chen, Z. Wang, J. Y. Fan, Q. Zhang, and J. W. Pan, “Quantum teleportation with independent sources over an optical fibre network,” Nat. Photonics **10**, 671–675 (2016).
5. R. Alléaume, F. Treussart, J. M. Courty, and J. F. Roch, “Photon statistics characterization of a single-photon source,” New J. Phys. **6**, 85 (2004).
6. A. Beveratos, R. Brouri, T. Gacoin, A. Villing, J. P. Poizat, and P. Grangier, “Single photon quantum cryptography,” Phys. Rev. Lett. **89**(18), 187901 (2002).
7. S. Kako, C. Santori, K. Hoshino, S. Götzinger, Y. Yamamoto, and Y. Arakawa, “A gallium nitride single-photon source operating at 200 K,” Nat. Mater. **5**(11), 887–892 (2006).
8. I. Aharonovich, D. Englund, and M. Toth, “Solid-state single-photon emitters,” Nat. Photonics **10**(10), 631–641 (2016).
9. L. A. Ngah, O. Alibart, L. Labonte, V. D’Auria, and S. Tanzilli, “Ultra-fast heralded single photon source based on telecom technology,” Laser Photonics Rev. **9**(2), 2 (2015).
10. M. Bock, A. Lenhard, C. Chunnilall, and C. Becher, “Highly efficient heralded single-photon source for telecom wavelengths based on a PPLN waveguide,” Opt. Express **24**(21), 23992–24001 (2016).
11. S. Fasel, O. Alibart, S. Tanzilli, P. Baldi, A. Beveratos, N. Gisin, and H. Zbinden, “High-quality asynchronous heralded single-photon source at telecom wavelength,” New J. Phys. **6**, 163 (2004).
12. S. Takeuchi, R. Okamoto, and K. Sasaki, “High-yield single-photon source using gated spontaneous parametric downconversion,” Appl. Opt. **43**(30), 5708–5711 (2004).
13. X. S. Ma, T. Herbst, T. Scheidl, D. Wang, S. Kropatschek, W. Naylor, B. Wittmann, A. Mech, J. Kofler, E. Anisimova, V. Makarov, T. Jennewein, R. Ursin, and A. Zeilinger, “Quantum teleportation over 143 kilometres using active feed-forward,” Nature **489**(7415), 269–273 (2012).

#286799 https://doi.org/10.1364/OE.25.012493
Journal © 2017 Received 15 Feb 2017; revised 7 May 2017; accepted 9 May 2017; published 19 May 2017

Optics EXPRESS

14. A. Trifonov and A. Zavriyev, "Secure communication with a heralded single-photon source," J. Opt. B. **12**, 7 (2005).
15. S. Castelletto, I. P. Degiovanni, A. Migdall, and V. Schettini, "Spatial and spectral mode selection of heralded single photons from Parametric Down-Conversion in bulk and PPLN," Proc. SPIE **5893**, 589315 (2005).
16. X. Chen, J. Shi, Y. Chen, Y. Zhu, Y. Xia, and Y. Chen, "Electro-optic Solc-type wavelength filter in periodically poled lithium niobate," Opt. Lett. **28**(21), 2115–2117 (2003).
17. R. H. Brown and R. Q. Twiss, "A test of a new type of stellar interferometer on Sirius," Nature **178**(4541), 1046–1048 (1956).
18. R. Loudon, *The Quantum Theory of Light* (Oxford University, 1983).
19. M. J. Collins, C. Xiong, I. H. Rey, T. D. Vo, J. He, S. Shahnia, C. Reardon, T. F. Krauss, M. J. Steel, A. S. Clark, and B. J. Eggleton, "Integrated spatial multiplexing of heralded single-photon sources," Nat. Commun. **4**, 2582 (2013).

## 1. Introduction

The single-photon source (SPS) plays a key role in research fields such as quantum computing and communication, especially in quantum key distribution (QKD) [1,2]. Multi photons can compromise the security of the communication by allowing eavesdroppers to steal information. In principle, for the same secure communication rate, single-emitter-based QKD systems can achieve longer key transmission distances than faint-laser pulse systems [3,4]. So far, several schemes for SPS have been proposed, which are mainly divided into two categories: 1. Color centers, quantum dots, single atoms, single ions and atomic ensembles are considered as deterministic SPS [5–8]; 2. Photons created in pairs via four-wave mixing in fibers and spontaneous parametric down conversion (SPDC) in bulk crystals and waveguides are described probabilistic one, which is called heralded single-photon source (HSPS) [9–13]. SPS have been continuously improved in purity, efficiency, repetition rate and usability in the past decade. However, deterministic SPSs are currently unsuitable for practical applications. For instance, the emitted photons are in visible spectrum, which is not compatible with existing telecommunication networks. Furthermore, the operating temperature of currently available SPSs is quite low. Therefore, the HSPS by SPDC is widely used in the field of quantum communication. Considering the excellent security of quantum communications, it is important to build quantum communication networks [14]. Such networks will require multipoint links, for which the point-to-multipoint SPS is an essential component.

Here, we report on the realization of a high efficiency multiple-channel HSPS at telecom wavelength through SPDC with a periodically poled lithium niobate (PPLN) waveguide. In brief, it is a point-to-multipoint HSPS. The efficiency of SPDC in waveguide is several times higher than the one in bulk, which ensures high repetition rate in each channel. Our source covers over forty 100-GHz dense wavelength division multiplexer (DWDM) ITU grid channels and each channel contains almost the same brightness and high quality. In addition, all fiber setup makes our source a good choice for quantum networks.

## 2. Theory and experiment setup

In our HSPS experiment, the nonlinear crystal to generate daughter photon pairs is a type-0 PPLN waveguide, which has the relatively large $\chi^{(2)}$ optical nonlinearity [15, 16]. The high efficient process of SPDC should meet the quasi-phase matching (QPM) conditions, i.e., $\vec{k}_p = \vec{k}_s + \vec{k}_i + \vec{k}_\Lambda$ and $\omega_p = \omega_s + \omega_i$, where $p, s, i$ denote pump, signal and idler waves, respectively. $k$ and $\omega$ are the wavevector and the frequency of the waves. We simulate the efficiency of the SPDC with Sellmeier equation, with pump wavelength at 777.88 nm. The spectrum of the SPDC output is resolved using a diffraction grating spectrometer (Shamrock, Andor) with a wavelength resolution of about 1 nm. The photons are detected by a single photon detector. The result in Fig. 1(a) shows an ultra-wide QPM bandwidth with a full width at half maximum (FWHM) of approximate 70 nm. This special property is basic to our multiple-channel source. The discrepancy between the theoretical and experimental results

Optics EXPRESS

mainly results from the error of empirical values in the Sellmeier equation and the waveguide dispersion.

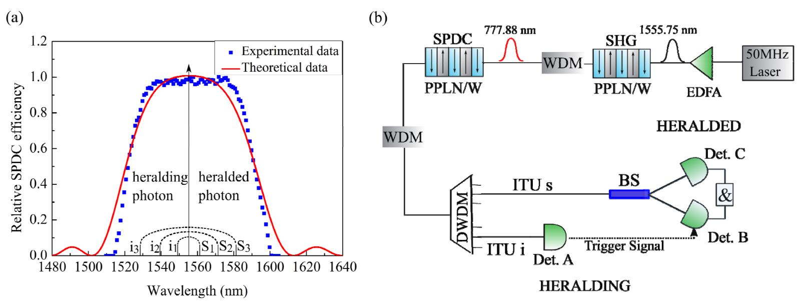


Fig. 1. (a) The red curve is the simulation of SPDC efficiency of our PPLN waveguide. The FWHM is 70 nm, which covers part of S-band, L-band and whole C-band. $s_n$ and $i_n$ ( $n = 1,2,3$ ) are daughter photon pairs, which represent CH26-CH24 and CH28-CH30 in the experiment, respectively. The $i_n$ are used as heralding photons to trigger the $s_n$ ones. (b) Schematic of multi-channel heralded single-photon source (EDFA: erbium doped fiber amplifier, WDM: 780-1560 nm wavelength division multiplexer, DWDM: dense wavelength division multiplexing, BS: fiber beam splitter, Det.: InGaAs single photon detector).

The experimental setup of our source is shown in Fig. 1(b). The laser at telecom wavelength (KG-PLS5011, CONQUER) with a repetition rate of 50MHz is first amplified to 120 mW by an EDFA (GA3210-23, CONNET), and then it's wavelength is converted to near infrared region by second harmonic generation (SHG) in the first PPLN waveguide, which is used as a pump for spontaneous parametric down conversion through the second PPLN waveguide. The pump has a maximum power of 8 mW with 1.0 ns pulse duration. Both of the processes take place in PPLN waveguides (SH-50-PM-SM-2-2, SIQST) with type-0 phase-matching condition. The temperature of PPLN is controlled at 325.4 ± 0.1 K. At the output of SPDC, a high-isolation WDM is used to filter the pump laser. The photon pairs are then split by a 100-GHz DWDM, which has seven channels within the ITU grid (CH24 - 30). The short-wavelength photon is defined as heralding photon and detected by Detector A directly. The long-wavelength one propagating through a 50/50 fiber optical beam splitter is considered the heralded single photon and is detected by Detector B and Detector C, which are trigged by Detector A. Two output ports of the detectors are connected to a photon correlator (DPC-230, Becher & Hickl GmbH) to measure the coincidence. This system is referred to as a Hanbury Brown-Twiss interferometer [17].

The three detectors (SPD4F100A, ROI. OP) are all InGaAs APDs operated in gated mode and the gate-width is 1.0 ns. We keep overall detection efficiencies $\beta$ 's at 10.0 ± 0.2%, thus the dark count probabilities per gate are $d_A = 11.6\times10^{-6}$ , $d_B = 8.3\times10^{-6}$ and $d_C = 10.0\times10^{-6}$ respectively. We set the internal triggering rate of Detector A at 50 MHz with a 5-μs deadtime, in which after-pulse counts are negligible. The other two detectors are set in external trigger mode with a 5-μs deadtime. The isolation of WDM at 780 nm reaches up to 120.0 dB, with only 2.0 dB loss at 1550 nm. The loss of DWDM is 1.8 dB each channel averagely. The coupling ratio of the waveguide is about 60%, equaling 2.2 dB.

By definition, an SPS is ideal when its probability of emitting a single photon is 100%, and the probability of multi-photon emission is 0% at any time. The photon source can be characterized with the $g^{(2)}(\tau)$ parameter of second-order correlation function [18]. In our setup, the $g^{(2)}(\tau)$ is equal to [11]:

Optics EXPRESS

$$g^{(2)}(\tau) = \frac{p_{BC}}{p_B \cdot p_C}, \tag{1}$$

where $\tau$ is the delay time between Detector B and C, $p_B$ and $p_C$ are the probabilities of detection coincidence of Detector A, Detector B and Detector A, Detector C respectively. $p_{BC}$ is the probability of having detection coincidences among all three detectors. These three probabilities are defined as:

$$p_B = \frac{N_B}{N_t}, \quad p_C = \frac{N_C}{N_t}, \quad p_{BC} = \frac{N_{BC}}{N_t}, \tag{2}$$

where $N_B$ and $N_c$ are the count of the given detector per second. $N_{BC}$ is the number of a simultaneous detection of both detectors. $N_t$ is the number of acquisition triggers.

For an ideal SPS, the parameter $g^{(2)}(0) = 0$, with $g^{(2)}(\tau) > g^{(2)}(0)\ (\tau \neq 0)$. Besides of $g^{(2)}(\tau)$, $P(1)$ and $P(2)$ are two other crucial parameters for the HSPS, which are relevant to $g^{(2)}(\tau)$. $P(1)$ is the probability of generating exactly one photon per heralding signal, while $P(2)$ is the probability of generating more than one photon. According to the equation $P(0) + P(1) + P(2) = 1$, the larger $P(1)$ the better and just the opposite for $P(2)$. Given that the Hanbury Brown-Twiss interferometer cannot distinguish between two and more photon events and $P(n)(n > 2) << P(2)$, we classify $P(n)(n \geq 2)$ as $P(2)$. The expressions of $P(1)$ and $P(2)$ are given by:

$$P(1) = \frac{p_B + p_C}{\beta}, \quad P(2) = 2\frac{p_{BC}}{\beta^2}, \quad g^{(2)}(\tau) \cong \frac{2P(2)}{P(1)^2}, \tag{3}$$

where the expressions of $P(1)$ and $P(2)$ are simplified in case $p(2) << p(1)$ and $d_B = d_C = 0$. The parameter $g^{(2)}(0)$, $P(1)$ and $P(2)$ are measured and analyzed in our experiment. They accurately reflect the quality of our source.

## 3. Experiment results

To ensure the quality of the photon pair from SPDC, the coincidence-to-accidental ratio (CAR) was measured, firstly. The CAR is the quality merit for characterizing the signal-to-noise ratio of photon pair [19]. The CAR is expressed as:

$$CAR = \frac{C}{\left(\frac{C}{\eta_s} + d_i\right)\left(\frac{C}{\eta_i} + d_s\right)}, \tag{4}$$

where $C$ is the coincidence per detection gate, $\eta_s$ and $\eta_i$ are the efficiencies of signal and idler channels, which are determined by the total losses in each channel. The losses mainly result from WDM, DWDM, detectors and connecting loss in fiber. They are listed in Table 1. Parameters $d_i$ and $d_s$ are the dark count rates per gate, which have been introduced above. Figure 2 shows the relationship between pump's power and CAR.

**Table 1. Total losses in each channel**

| Channel | 24 | 25 | 26 | 28 | 29 | 30 |
|---|---|---|---|---|---|---|
| Total loss (dB) | 16.4 | 16.5 | 16.7 | 16.1 | 16.7 | 16.6 |

Figure 2 shows that the CAR is less than 10 when the pump power is over 31.80 μW. CAR's best performance interval ranges between 0.27 μW and 3.18 μW. It drops sharply as long as the power is under 0.22 μW, because dark count dominates in the data count. In addition, taking the brightness of the source into consideration, we set the pump's power from 1.06 μW to 23.85 μW. CAR distributes from 175 to 11. In other words, the quality and brightness of each HSPS's channel is relatively good under these circumstances.

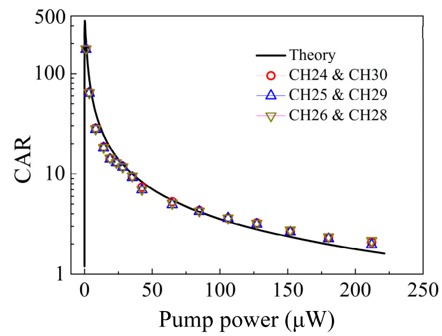


Fig. 2. CAR for three daughter pairs.

In our experiment, the heralding rate $R_H$ can reach 68 kHz at 23.85 μW. The dark count has been subtracted in all data. $P(1)$ and $P(2)$ are calculated from the raw data. We figure out $P_{24}(1) = 0.23 \pm 0.01$ , $P_{25}(1) = 0.22 \pm 0.01$ and $P_{26}(1) = 0.21 \pm 0.01$ [Fig. 3(a)]. Comparing with the losses (without detection efficiency) in these three channels ($l_{24} = 6.4$ dB, $l_{25} = 6.5$ dB, $l_{26} = 6.7$ dB), we draw the conclusion that $P(1)$ is a good approximation by the propagation efficiency in a certain channel. In this experiment, $P_x(1)$ is constant and equals:

$$P_x(1) = T_C \cdot T_{WDM} \cdot T_{DWDM} \cdot T_{BS} \cdot T_{Fiber}, \tag{5}$$

where $T_C$, $T_{WDM}$, $T_{DWDM}$, $T_{BS}$ and $T_{Fiber}$ are the transmissions of coupler, WDM, DWDM, BS and all fibers, respectively. This provides us with an idea that if the losses of these devices were reduced, $P(1)$ would increase directly. Perfect $P(1)$ could rise up to 0.6, limited by the coupling ratio of the waveguide. In theory, $P(2)$ and $g^{(2)}(0)$ can be expressed as [12]:

$$P(2) = \frac{1}{2} \cdot P(1)^2 \cdot \Delta t \cdot \eta_p \cdot \overline{P}_p, \tag{6}$$

$$g^{(2)}(0) \approx \Delta t \cdot \eta_p \cdot \overline{P}_p, \tag{67}$$

where $\Delta t$ is the duration of the detector gate, $\eta_p$ is the pair creation efficiency of the PPLN waveguide and $\overline{P}_p$ is the pump power. From Eqs. (6) and (7), $P(2)$ and $g^{(2)}(0)$ can be arbitrary low by decreasing the pump power and $g^{(2)}(0)$ is independent of $P(1)$. Figure 3(a) shows that $g^{(2)}(0)$ is proportional to $\overline{P}_p$, which is in accordance with theoretical results. Beyond that, the three channels behave almost identically under the same pump power, such as heralding rate, $P(1)$, $P(2)$ and $g^{(2)}(0)$. This unique property makes our source a stable and controllable point-to-multipoint HSPS. At the highest heralding rate of 67 kHz, the $g^{(2)}(0)$ is around 0.13. The $g^{(2)}(0)$ falls to lower than 6.7 × $10^{-3}$ at 1.06 μW pump power (heralding rate 5 kHz). We compare these results to a Poissonian light source [ $g^{(2)}(0) = 1$ ] featuring the

Optics EXPRESS

same value for $P(1)$. Mainly the multi-photon emission probability $P(2)$ of each channel is reduced by the factor $1/g^{(2)}(0)$ ranging from around 7.5 to over 150.

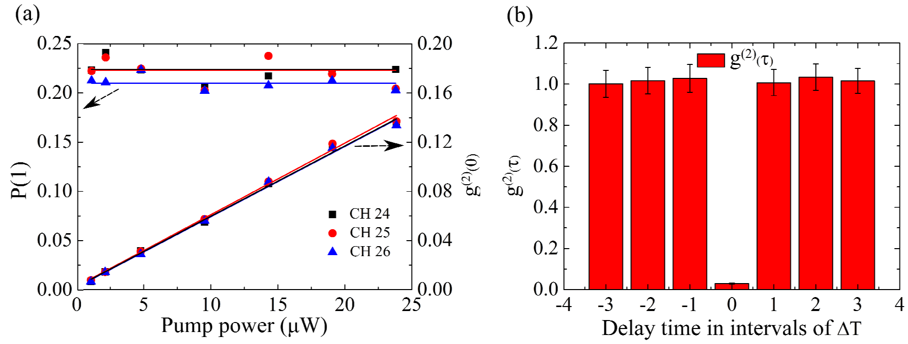


Fig. 3. (a) Measured the relationship between $P(1)$ and pump power; Measured $g^{(2)}(0)$ as a linear function of the pump power. (b) The relationship between $g^{(2)}(\tau)$ and delay time. The pump power is 4.77 μW and collection time is 600 s. Our detectors can delay the gate with the accuracy of 0.01 ns. In this case, the interval of delay-time $\tau$ is 20 ns.

Figure 3(b) shows the relationship between $g^{(2)}(\tau)$ and delay time. Evidently, $g^{(2)}(\tau)$ reaches 1 directly when $\tau$ is equal to mT, where T is the periodic time of the pump 20 ns and m is nonzero integer.

In comparison with other recent implementations of HSPSs [9], our source contains more number of channels. A low rate of multi-photon emission in each channel is also achieved. The repetition rate of the laser has little influence on the SPDC efficiency or the phase-matching condition. Thus, the spectral content and spectral extent of the SPDC photons will not change significantly if the bandwidth of the pump is the same for lasers with different repetition rates. Considering that the value of the $R_H$ directly depends on the repetition rate of the laser and the detection efficiency, an ultra-fast multiple-DWDM-channel heralded single-photon source can be realized by improving the laser and detectors without introducing any degradation to the value of $g^{(2)}(0)$.

## 4. Conclusion

In conclusion, we have demonstrated and characterized a multi-DWDM-channel HSPS with high quality. We realize a multi-channel HSPS with the pump power lower than 23.85 μW. Each heralded channel has nearly constant $P(1)$ about 0.22. The measured second-order correlation function $g^{(2)}(0)$ ranges from $6.7 \times 10^{-3}$ to 0.13. For the best $g^{(2)}(0)$, it is suppressed by a factor of more than 150 relative to the classical light. We demonstrate that a PPLN waveguide setup can be used to implement a high quality multiple-DWDM-channel heralded single-photon source. We explore each channel's performance for different pump powers. In a practical application, good tradeoffs between low $g^{(2)}(0)$ and high brightness can be guaranteed. Furthermore, our source is all fiber structure at room temperature without cooling. It is therefore an ideal candidate for real-world quantum networks.

## Funding

National Natural Science Foundation of China (Grant No. 61235009).